A glucose sensor hiding in a family of transporters

Ana Díez-Sampedro*, Bruce A. Hirayama*, Christina Osswald†, Valentin Gorboulev†, Katharina Baumgarten†, Christopher Volk†, Ernest M. Wright*‡, and Hermann Koepsell†

*Department of Physiology, David Geffen School of Medicine, University of California, 10833 Le Conte Avenue, Los Angeles, CA 90095-1751; and †Anatomical Institute, University of Wurzburg, Koellikerstrasse 6, 97070 Wurzburg, Germany

Edited by Michael J. Welsh, University of Iowa College of Medicine, Iowa City, IA, and approved July 2, 2003 (received for review May 20, 2003)

We have examined the expression and function of a previously undescribed human member (SGLT3/SLC5A4) of the sodium/glucose cotransporter gene family (SLC5) that was first identified by the chromosome 22 genome project. The cDNA was cloned and sequenced, confirming that the gene coded for a 659-residue protein with 70% amino acid identity to the human SGLT1. RT-PCR and Western blotting showed that the gene was transcribed and mRNA was translated in human skeletal muscle and small intestine. Immunofluorescence microscopy indicated that in the small intestine the protein was expressed in cholinergic neurons in the submucosal and myenteric plexuses, but not in enterocytes. In skeletal muscle SGLT3 immunoreactivity colocalized with the nicotinic acetylcholine receptor. Functional studies using the *Xenopus laevis* oocyte expression system showed that hSGLT3 was incapable of sugar transport, even though SGLT3 was efficiently inserted into the plasma membrane. Electrophysiological assays revealed that glucose caused a specific, phlorizin-sensitive, Na^+-dependent depolarization of the membrane potential. Uptake assays under voltage clamp showed that the glucose-induced inward currents were not accompanied by glucose transport. We suggest that SGLT3 is not a Na^+/glucose cotransporter but instead a glucose sensor in the plasma membrane of cholinergic neurons, skeletal muscle, and other tissues. This points to an unexpected role of glucose and SLC5 proteins in physiology, and highlights the importance of determining the tissue expression and function of new members of gene families.

Na/sugar cotransporter | human SGLT3 | muscle

Glucose, in addition to its central role in metabolism, also plays an important role as a signaling molecule in animal and plant cells (1). Glucose sensing is critical to such diverse physiological phenomena as regulation of metabolism in yeast, photosynthesis in higher plants, and, in mammals, the regulation of food intake, blood glucose levels, and enteric reflexes. Apart from yeast, where homologs of facilitated glucose transporters (Snf3 and Rgt2) have been implicated in glucose sensing (2), little is known about the molecular mechanisms involved. In this study we have cloned and examined the tissue localization and function of a member of the large Na^+/glucose cotransporter family, hSGLT3, and the results suggest that it is a glucosensor in smooth and skeletal muscle.

Human members of the SLC5 gene family include the intestinal and renal glucose transporters (SLC5A1, SLC5A2), the widely distributed inositol and multivitamin transporters (SLC5A3, SLC5A6), and the thyroid iodide transporter (SLC5A5). Although a major function of these plasma membrane proteins is secondary active transport in epithelia, they also behave as Na^+ uniporters, water and urea channels, and water cotransporters (3, 4). We have previously demonstrated that a pig SGLT3 expressed in *Xenopus laevis* oocytes also behaves as tightly coupled Na^+/glucose cotransporter with a lower affinity for glucose and a more restricted sugar specificity than SGLT1 (SLC5A1) clones (5–8). The human homolog to pig SGLT3 (hSGLT3, SLC5A4) was identified in the sequencing of chromosome 22 (9), and this prompted us to isolate the cDNA and confirm that it is indeed a Na^+/glucose cotransporter. Here we report that hSGLT3 is expressed in tissues such as smooth and skeletal muscle, and that hSGLT3 is not a coupled Na^+/glucose cotransporter but instead a glucosensor. These results suggest that hSGLT3 plays a hitherto unexpected role in regulating the activity of smooth and skeletal muscles, and underscore the importance of determining the cellular expression as an important clue to the physiological function of human genes.

Methods

Cloning hSGLT3. Initial RT-PCR was carried out on total RNA from a human colon carcinoma that expresses hSGLT3 (10). The primers were HSA6, designed from a known fragment of hSGLT3 (11) (forward, 5′-AGGTTATGAGAGCTTTAC-3′, position of 697–717, GenBank accession no. U41897) and a degenerate primer SA-DEG designed from a conserved region of the SGLT family (reverse, 5′-CCA(TC)AANGG(TC)TT-(TC)TCNGANGT(AG)TC-3′, position 1901–1924 of hSGLT3). The 1,228-bp fragment obtained was sequenced, and used to obtain the 3′ end of hSGLT3 by 3′ RACE using RNA from colon carcinoma as a template. The 5′ end was obtained by using PCR on colon carcinoma cDNA and 5′ RACE on Marathon-Ready intestinal cDNA (Clontech). An additional PCR was made to cover nucleotides 8–1,878 of hSGLT3. The complete hSGLT3 clone was created by ligation of this PCR product to the 3′-end of hSGLT3 at the *Hin*dIII site and cloned into plasmid pRSSP (kindly provided by R. Schopfer, Heidelberg, Germany). The cDNA used for functional studies in oocytes was resequenced and the predicted amino acid sequence was identical to that obtained in the genome project (9).

RT-PCR (12) was carried out on mRNA from human tissues (Clontech). Five different hSGLT3 primers were used: HSA40 forward, 5′-CTCGCTGGTCGTGATATGGCC-3′, position 194–214; HSA39 reverse, 5′-GCCAACATCAACGCCA-CAGTG-3′, position 1076–1096; HSA38 forward, 5′-GGGA-CAACTTGACAATCAGTGCC-3′, position 753–775; HSA37 reverse, 5′-TAGAGTTCAGGCATAGTAGCCG-3′, position 1981–2002; HSA42 forward, 5′-GTCAGGAAGAAACAGAT-GATGGTG-3′, position 1752–1775, and we used primer pairs separated by introns (9). The PCR products were resolved on agarose gels, blotted and hybridized with [γ-^{32}P]ATP-labeled oligonucleotides.

Immunohistochemistry. The hSGLT3 specific antibody was raised in rabbits against a peptide (EEKSQEETDDGVEEDY-PEKS-C, residues 576–595), and affinity purified (Sulfolink, Pierce). BLAST searches of the SWISS-PROT database using the peptide sequence failed to identify other proteins containing this peptide sequence, including nicotinic acetylcholine receptors (see below). The frozen tissue sections, fixed with 3% paraformaldehyde, were incubated for 1 h at 22°C with the antibody. The reaction of the anti-hSGLT3 antibody was detected with Cy3-coupled secondary antibody against rabbit IgG. The monoclonal

This paper was submitted directly (Track II) to the PNAS office.

Abbreviation: αMDG, α-methyl-D-glucopyranoside.

‡To whom correspondence should be addressed. E-mail: ewright@mednet.ucla.edu.

antibody for the human AchR β-subunit was from Acris (Hiddenhausen, Germany), and the reaction with acetylcholine receptor was visualized with Cy2-coupled secondary antibody against mouse IgG F(ab′)2 fragment. Both secondary antibodies were raised in goat (Dianova, Hamburg, Germany).

The human tissue used for immunohistochemistry and Western blotting was obtained in accordance with German law under the rules of the Ethics Commission of the University of Wurzburg. Both the duodenal sample (from a 50-year-old male gastrectomy patient) and the musculus rectus femoris sample (from a 35-year-old tumor patient) were tissues left over from the usual and customary pathological investigations.

Expression of hSGLT3 in Oocytes. Stage VI oocytes from *X. laevis* (Nasco, Fort Atkinson, WI) were defolliculated and injected with hSGLT3 cRNA and maintained at 18°C in modified Barth's medium containing gentamycin (5 mg/ml) and penicillin (100 units/ml)/streptomycin (100 μg/ml). Each oocyte was injected with 20 ng of cRNA. Experiments were performed at 22 ± 1°C, 3–9 days after the injection.

Western Blotting. Oocytes were incubated for 3 days after cRNA injection. Plasma membranes from oocytes or tissues were isolated (13) and probed as described (14). Whole tissue samples were homogenized in 280 mM sucrose, 20 mM Tris·HCl (pH 7.5), 5 mM EGTA, 5 mM $MgSO_4$, and 1 mM PMSF and centrifuged at 8°C for 10 min at 2,000 × *g*. Membranes were collected by centrifuging the supernatant for 60 min at 40,000 × *g*. The resulting pellet was used for Western blotting. Oocyte membranes were homogenized in 10 mM Hepes (pH 7.9), 83 mM NaCl, 1 mM $MgCl_2$ containing 1 mM PMSF, 0.5 μg/ml aprotinin, 0.05 μg/ml leupeptin, and 10 mM benzamidine. Debris was removed by centrifugation at 1,000 × *g*, and membranes were collected from the supernatant by centrifugation for 20 min at 10,000 × *g*. The hSGLT3 antibody dilution was 1:1,000 (serum) and the secondary antibody was peroxidase-labeled goat anti-rabbit IgG, and was detected by chemical luminescence (Amersham Pharmacia). The β-subunit AchR antibody was used according to the supplier's recommendations. Specificity of the hSGLT3 antibody reaction was verified by showing that no immunohistochemical reaction was observed when the antibodies had been blocked by a 1-h (37°C) incubation with 0.1 mg/ml antigenic peptide. The β-subunit AchR antibody did not immunoreact with hSGLT3 expressed in oocytes.

Two-Electrode Voltage Clamp. Oocytes expressing SGLTs and control oocytes were placed in the chamber, impaled with the two electrodes and continuously superfused with the required medium (15). Membrane potential changes and ionic currents were measured when adding different sugar concentrations. Sugar-specific changes in current were the difference between the values measured with sugar and the preceding value in buffer alone. Na^+ buffer contained 100 mM NaCl, 2 mM KCl, 1 mM $CaCl_2$, 1 mM $MgCl_2$, and 10 mM Hepes/Tris (pH 7.5). In Na^+-free buffer, choline Cl replaced NaCl, and for the experiments at pH 5.0, Hepes/Tris was replaced with Mes/Tris. In some experiments at low pH, we simultaneously recorded the intracellular pH of the oocyte by using the fluorescent dye BCECF-AM (15, 16). The apparent affinity ($K_{0.5}$) and apparent maximal current (I_{max}) were calculated with the equation $I = I_{max} \cdot [S]/(K_{0.5} + [S])$, using the nonlinear fitting method in SIGMAPLOT (SPSS, Chicago), where [S] is the sugar concentration. The results are illustrated by experiments on single oocytes, but each was representative of three to eight different oocytes.

Uptake Experiments. Control oocytes or oocytes expressing a SGLT were superfused with a buffer solution containing either 100 mM NaCl or choline chloride at pH 7.5 or 5, and the plasma membrane potential was clamped at voltages between −50 and −110 mV. When the baseline was stable, D-glucose with tracer [^{14}C]glucose was added. After the sugar was removed from the bathing solution, the current returned to the baseline. The oocyte was washed and solubilized, and glucose uptake was determined by using a scintillation spectrometer. Sugar-induced current was obtained by integrating the difference between baseline and the glucose-dependent current. The current, measured simultaneously with sugar uptake, was converted to its molar equivalent of univalent charge. [^{14}C]Glucose uptake in noninjected oocytes from the same batch of oocytes was used as a control (8)

Results

Human SGLT3 was identified as a member of the SLC5 gene family by the chromosome 22 genome project (GI:5679464) (9). The cDNA was cloned and sequenced (GI:7263938). The amino acid sequence of the 659 residue protein is identical to that deduced from the genomic sequence. It has 82% amino acid identity to the pig SGLT3 (previously called SAAT1, ref. 17), and 70% identity to human SGLT1 Na^+/glucose cotransporter (18). To gain insight into the role of hSGLT3 we examined where the gene is transcribed and the protein is expressed. Northern blotting and PCR have detected SGLT3 mRNA in pig kidney, intestine, skeletal muscle, and spleen (17). When we used RT-PCR, we also detected SGLT3-RNA in human skeletal muscle and small intestine. Fig. 1*A* shows that the mRNA was present in both tissues by using different primers. Each primer pair amplified the predicted DNA product from both intestinal and skeletal muscle RNAs. In other experiments, RNase protection assays showed that hSGLT3 was also transcribed in kidney, uterus, and testis (data not shown).

Western blots demonstrated that hSGLT3 mRNA was translated in the human small intestine and skeletal muscle (Fig. 1*B*). A ≈60-kDa band was detected in plasma membranes from oocytes injected with hSGLT3 cRNA (lane 4) and not in the ones injected with hSGLT1 cRNA (lane 5), showing the specificity of the antibody. The antibody identified an identical band in samples from whole small intestine (lane1) and skeletal muscle plasma membranes (lane 3), and in all cases the immunoreactivity was blocked by the hSGLT3 peptide.

Confocal immunofluorescence microscopy (Fig. 2*A*) revealed that the hSGLT3 protein in the intestine (red) was restricted to discrete patches of the plasma membrane of cells in the submucosa (*A1*) and in the longitudinal smooth muscle cells (*A4*), but no immunoreactivity was detected in the enterocyte. In both locations, the immunoreactively was blocked by the hSGLT3 peptide, and the hSGLT3 immunoreactivity colocalized with the β-subunit of the nicotinic acetylcholine receptor (*A2* and *A5*, the receptor shown in green, and *A3* and *A6*, the superimposed images in yellow). These results suggest that, in the intestine, hSGLT3 is expressed in cholinergic neurons of the submucosal plexus and myenteric plexus (Fig. 2*B*). In skeletal muscle, hSGLT3 is detected in discrete regions of the plasma membrane (Fig. 3*A*) and colocalized with the acetylcholine receptor (Fig. 3*B*), suggesting that hSGLT3 is at the neuromuscular junction. The resolution does not permit us to conclude whether hSGLT3 is expressed in the pre- or postsynaptic membrane of the junction.

What role does hSGLT3 play in the physiology of cholinergic neurons and muscle? To address this question, we examined functional properties of hSGLT3 in the *X. laevis* oocyte expression system by using biochemical and biophysical techniques. Western blots demonstrated that the cRNA injected into the oocytes was translated (Fig. 1*B*), and freeze-fracture electron microscopy (19) indicated that the protein was efficiently inserted into the plasma membrane (data not shown). Radioactive tracer assays, however, showed that hSGLT3 expressed in oo-

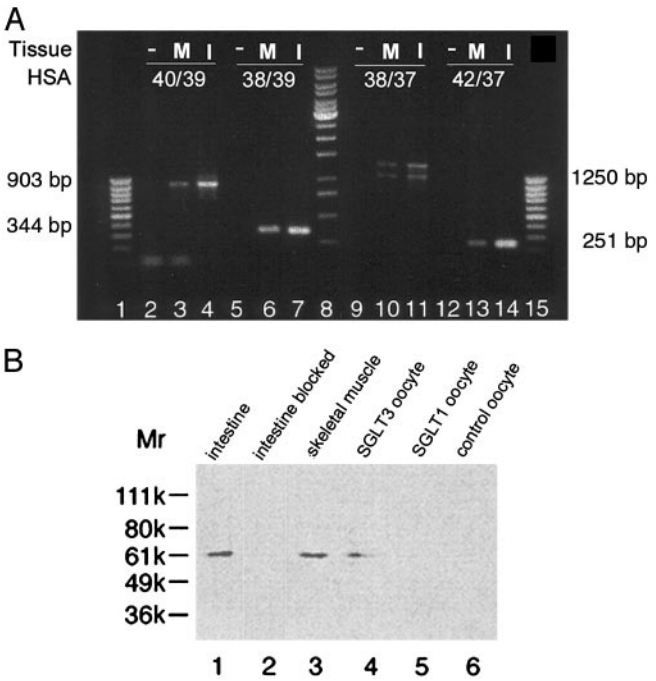

Fig. 1. (*A*) Identification of hSGLT3-mRNA in human skeletal muscle and human small intestine by RT-PCR. Several different pairs of primers were used: lanes 2–4, primer HSA40/primer HSA39 (segment size: 903 bp); lanes 5–7, primer HSA38/primer HSA39 (segment size: 344 bp); lanes 9–11, primer HSA38/primer HSA37 (segment size: 1,250 bp); lanes 12–14, primer HSA42/primer HSA 37 (segment size: 251 bp). The primer pairs are separated by introns of the genomic DNA. Lanes 1 and 15, 100-bp ladder (MBI Fermentas); lane 8, 1-kbp ladder (MBI Fermentas); lanes 2, 5, 9, and 12, negative controls (−) (water instead of RNA in RT-PCR); lanes 3, 6, 10, and 13, skeletal muscle (M); lanes 4, 7, 11, and 14, small intestine (I). The PCR products were resolved on agarose gel, blotted, and hybridized with hSGLT3-specific oligonucleotides ([γ-^{32}P]ATP) to verify the identification of hSGLT3. Amplificates HSA40/HSA39 and HSA38/HSA39 were hybridized with HSA27 (nucleotides 982–1,006, forward). Amplificates HSA38/HSA37 and HSA42/HSA37 were hybridized with HSA30 (nucleotides 1,878 to 1,855, reverse) (data not shown). (*B*) Immunochemical staining of Western blots with affinity-purified antibody against amino acids 576–595 from hSGLT3. Plasma membranes from the small intestine, skeletal muscle, and *Xenopus* oocytes were isolated by differential centrifugation (14). The oocytes were injected with 20 ng of hSGLT3-cRNA (lane 4), 20 ng of hSGLT1-cRNA (lane 5), or water (lane 6). In the Western blots, 20 μg of protein was applied per lane. The hSGLT3 antibody recognized a single protein band (≈60 kDa) in membranes isolated from whole small intestine (lane 1) and skeletal muscle (lane 3), and from oocytes injected with hSGLT3 cRNA (lane 4), but not from oocytes injected with cRNA from hSGLT1 (lane 5). Lane 2, membranes from small intestine again, but this time the antibody against SGLT3 was blocked by 1 h (37°C) incubation with 0.1 mg/ml antigenic peptide.

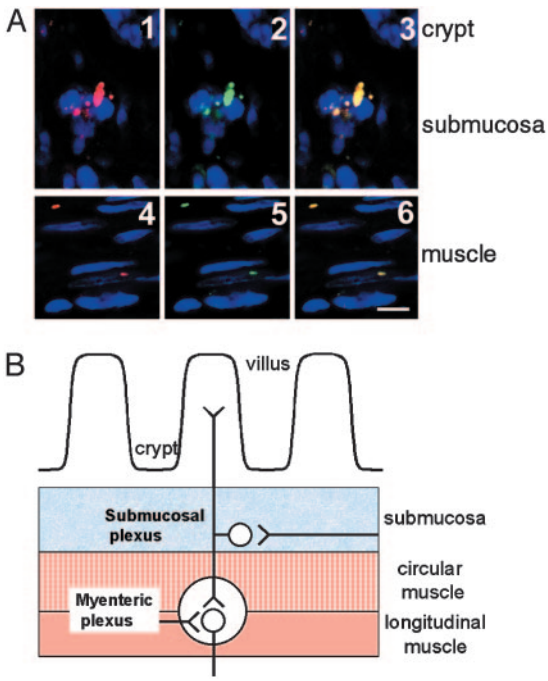

Fig. 2. (*A*) Laser-scanning confocal micrographs of immunostaining by the anti-hSGLT3 antibody (red, *1* and *4*) and anti-acetylcholine receptor β-subunit (green, *2* and *5*) in the intestine. The images were superimposed to show that the antibodies stain the same structure (yellow, *3* and *6*). Reaction products were found below villus crypts in the plexus submucosus (*1–3* cross section with crypt in the upper right), and in the plexus myoentericus (*4–6*, longitudinal section). (Scale bar = 10 μm.) (*B*) Cartoon of a cross-section of small intestine showing the major structures and location of the myenteric neurons.

cytes did not increase the uptake of glucose into oocytes over that of control, noninjected oocytes (described below).

Because freeze-fracture electron microscopy showed that hSGLT3 was inserted in the plasma membrane, we used the two-electrode voltage-clamp to monitor hSGLT3's electrical properties in *Xenopus* oocytes. Exposure of the oocytes expressing hSGLT3 to D-glucose (and the nonmetabolized analogue α-methyl-D-glucopyranoside, αMDG) reversibly depolarized the membrane potential (Fig. 4*A*). This depolarization was specific for D-glucose and αMDG, and was blocked by 250 μM phlorizin. Phlorizin is a specific competitive inhibitor of pig SGLT3 (6). D-galactose, D-fructose, and mannitol had no effect on the membrane potential at concentrations as high as 100 mM. The glucose-induced depolarization saturated with increasing glucose concentrations with an apparent K_m of 20 mM and the maximum depolarization (ΔV_m) was 23 mV (Fig. 4*B*). This suggests that glucose induced an ionic current through hSGLT3.

We measured the hSGLT3 currents in oocytes under voltage-clamp conditions and determined the effect of membrane po-

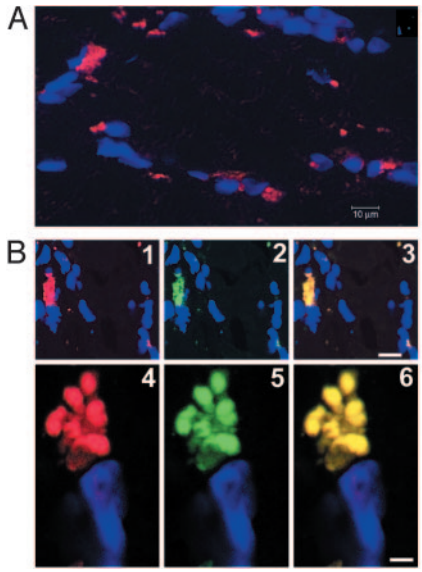

Fig. 3. (*A*) The reaction of hSGLT3 antibody in a human skeletal muscle biopsy. The nuclei are stained with 4′,6-diamidino-2-phenylindole (DAPI) (blue). (*B*) Immunostaining by the anti-hSGLT3 antibody (red, *1* and *4*) and the anti-acetylcholine receptor β-subunit antibody (green, *2* and *5*) in skeletal muscle. *3* and *6* show that both antibodies stain the same structure. (Scale bar = 10 μm in *3* and 2 μm in *6*.)

PHYSIOLOGY

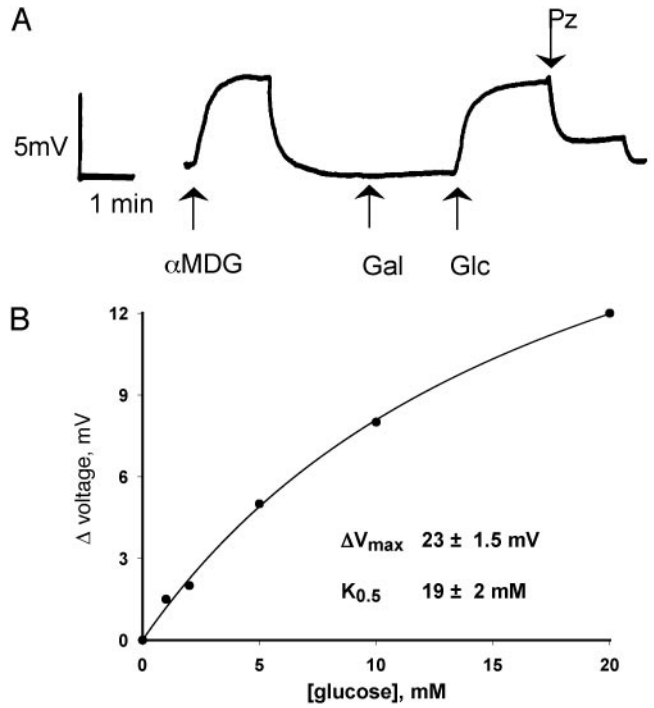

Fig. 4. Sugar-induced changes in membrane potential in a single hSGLT3-expressing oocyte. (*A*) In Na^+ buffer at pH 7.5, 5 mM glucose or αMDG depolarized the membrane by ≈4 mV, whereas 5 mM galactose had no effect. Phlorizin, a high-affinity competitive inhibitor of Na^+-glucose cotransport, at a concentration of 250 μM, inhibited the membrane depolarization induced by 5 mM glucose. (*B*) Voltage depolarization in response to glucose. The data were fitted to calculate the $K_{0.5}$ (≈20 mM glucose) and the maximal depolarization (23 mV) by using the equation $I = I_{max}\cdot[S]/(K_{0.5} + [S])$ (see text for details). In six experiments, $K_{0.5} = 60 \pm 10$ mM and $\Delta V_{max} = 26 \pm 9$ mV.

tential on the sugar-dependent current. Fig. 5 shows that αMDG-dependent hSGLT3 currents: (*i*) did not reverse at positive membrane potential; (*ii*) increased from +50 to −90 mV; and (*iii*) increased on lowering the pH to 5 in the presence or absence of Na^+. The sugar concentration dependence of the currents was also recorded. At −150 mV, the maximum current at the saturating sugar concentration (I_{max}) was 122 ± 20 nA ($n = 5$) and the apparent sugar affinity ($K_{0.5}$) was 36 ± 6 mM ($n = 5$). There were no sugar-induced currents in the absence of Na^+ indicating that Na^+ carried the inward current. In four of these oocytes at pH 5, the I_{max} was 1,725 ± 99 nA and the $K_{0.5}$ was 41 ± 7 mM at pH 5 in NaCl, and the I_{max} was 2,385 ± 651 nA and the $K_{0.5}$ was 131 ± 22 mM in choline Cl. These data indicate that H^+ carry the sugar current at pH 5, and this is supported by measurement of ^{22}Na uptakes and intracellular pH: there was no increase in Na^+ uptakes at pH 5, but there was a sugar-dependent acidification of the cytoplasm (Fig. 7, which is published as supporting information on the PNAS web site, www.pnas.org).

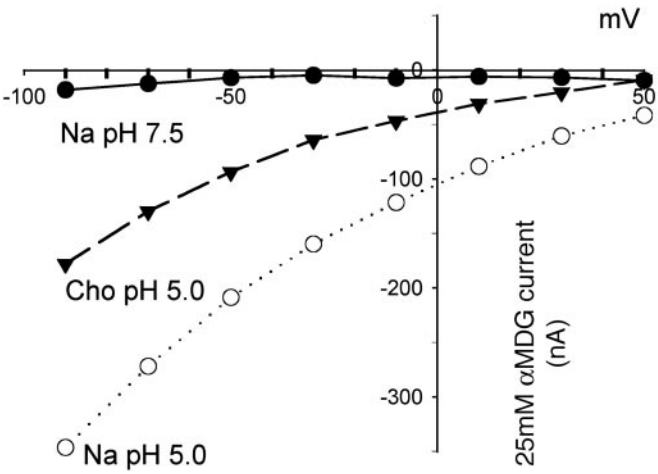

Fig. 5. Effect of membrane potential and pH on sugar-induced current in an hSGLT3-expressing oocyte. The figure shows the currents induced by 25 mM αMDG in Na^+ buffer at neutral and acidic pHs and in buffer without Na^+ at pH 5 at voltages ranging from +50 to −90 mV.

We examined the relationship between sugar and the inward ion currents through hSGLT3 by simultaneously measuring the radiotracer sugar uptake and sugar-induced currents. Sugar uptakes were identical in control oocytes and those expressing hSGLT3 in the absence or presence of Na^+ at pH 7.5 and 5. Fig. 6 illustrates experiments performed in oocytes in Na^+ at pH 5. After the baseline current was recorded in the absence of sugar, 2 mM D-glucose containing tracer [^{14}C]D-glucose was added and the sugar-induced currents were continuously recorded for 5 min. We compared uptake of glucose and the cation uptake (calculated from the integrated sugar-induced current as the net monovalent charge uptake) in each oocyte. D-Glucose uptakes were identical in hSGLT3 and control (noninjected) oocytes (11 ± 0.5 and 11 ± 0.6 pmol, $n = 5$, Fig. 6*B*). No cation uptakes were induced by glucose in control oocytes, whereas the cation uptake was 81 ± 7 pmol, $n = 5$ in hSGLT3 oocytes (Fig. 6*A*). With this cation uptake, we would expect a glucose uptake of 40 pmol if there were a 2/1 coupling between cation and sugar transport as in SGLT1. Because the glucose uptake did not increase above that of the control oocytes (Fig. 6*B*), we conclude that hSGLT3 is not a glucose cotransporter.

To validate these observations, we repeated the experiments with oocytes expressing hSGLT1 and pig SGLT3 (Fig. 6*C*). The results with both hSGLT1 and pig SGLT3 at pH 7.5 confirmed the 2/1 coupling between ion and sugar transport (8, 20). Whereas hSGLT1 remained strictly coupled at acid pH, pig SGLT3 became uncoupled at pH 5, i.e., the ratio of ion to sugar uptake increased to 5 (Fig. 6*C*).

The activation energy (E_a) for the sugar-induced hSGLT3 current was determined by measuring the glucose-induced currents in the presence and absence of Na^+ at pH 5 at 10, 22, and 28°C in the same oocyte. Arrhenius plots of the currents obtained in the presence and absence of Na^+ gave E_a values for the glucose-induced current of ≈9 kcal/mol, much lower than expected for cotransport (26 kcal/mol; ref. 3). To further characterize the glucose-induced currents through hSGLT3, we also recorded the effect of cytoplasmic pH on the I/V curves in the absence of Na^+ at an external pH of 5. In two experiments, we recorded the 100 mM αMDG currents from +50 to −150 mV before and after acidification of the cytoplasm by using a 50 mM K acetate pulse (data not shown). In both, the I/V curves shifted by −50 mV, similar to the D204N hSGLT1 mutant, which behaves as a glucose-gated ion channel (20). These results indicate that the sugar-induced currents through SGLT3 have properties more in common with channels than transporters.

Discussion

To determine the function of a new member of the SLC5 gene family, SGLT3, we have cloned the cDNA, determined where the gene is transcribed and the protein is expressed, and expressed the membrane protein in a heterologous expression system. The amino acid sequence encoded in the cDNA was identical to that predicted from the genomic sequence (9), and transcripts were detected in tissues including the small intestine and skeletal muscle. In the intestine, the protein is found in cholinergic neurons of the submucosal and myenteric plexuses

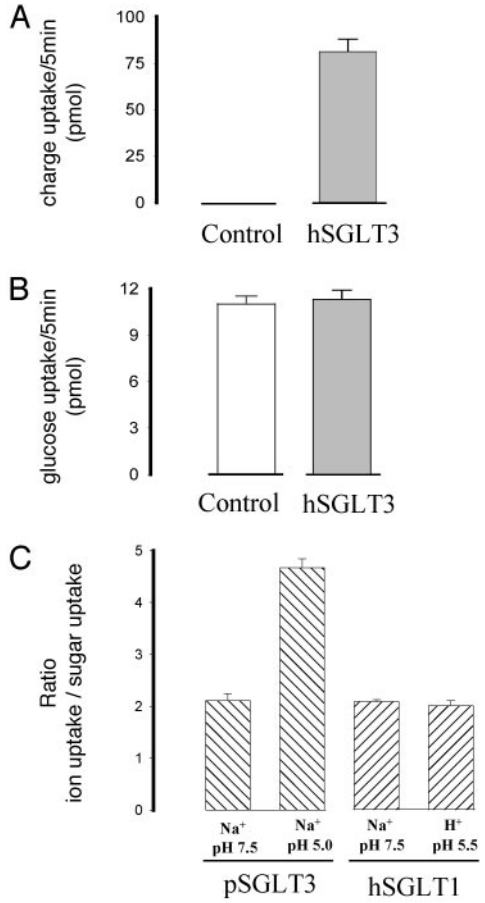

Fig. 6. Sugar uptake is not coupled to cation uptake through SGLT3. Sugar-induced current (*A*) and glucose uptake (*B*) were simultaneously measured in the same hSGLT3-expressing oocytes (hSGLT3) and in noninjected oocytes (control). The membrane was voltage-clamped at −70 mV, and the experiment was carried out in Na^+ buffer at pH 5. (*A*) In control oocytes, 2 mM glucose did not induce any current, whereas in hSGLT3-expressing oocytes, a sugar-dependent current equivalent to univalent positive charge of 81 ± 7 pmol per 5 min was recorded. (*B*) Glucose uptakes were recorded in the same oocytes used to measure the currents in *A*. The glucose uptake in the hSGLT3 oocytes was identical to that in control oocytes ($P > 0.5$). The data are from five hSGLT3-expressing and five control oocytes. (*C*) Ratio of positive ion uptake and sugar uptake in pSGLT3- and hSGLT1-expressing oocytes. These experiments were carried out as described for hSGLT3 (*A* and *B*). In hSGLT1-expressing oocytes, the ratio in Na^+ at neutral pH is 2.1 ± 0.04 ($n = 4$) and at acidic pH in H^+ is 2 ± 0.1 ($n = 7$) (taken from ref. 20). pSGLT3-expressing oocytes show the same ratio of positive charge/sugar uptake at neutral pH: 2.1 ± 0.1 ($n = 12$), but at acidic pH the ratio increases to 4.7 ± 0.2 ($n = 6$).

(see Fig. 2) and in skeletal muscle at the neuromuscular junction (Fig. 3). Unlike other members of the family, SGLT3 is not a glucose transporter when expressed in oocytes. However, glucose does produce a phlorizin-sensitive inward current that depolarizes the membrane potential by up to 50 mV. The low sugar affinity of the human SGLT3 at pH 7.5 (apparent affinity ≈60 mM) means that the depolarization in membrane potential is a linear function of glucose concentration in the physiological range (2–12 mM). We speculate that variations in plasma membrane glucose concentration modulate membrane potential in cholinergic neurons in the enteric nervous system and at the neuromuscular junction in skeletal muscle. The actual magnitude of the responses will depend on the density of SGLT3 proteins, the native conductance of the membranes, and whether SGLT3 is coupled to any other protein.

Intestinal motility in both rodents and man is finely regulated by the enteric nervous system, and all activity between and after a meal appears to be regulated by cholinergic neurons (21). The importance of glucose in regulating intrinsic enteric reflexes after a meal is well recognized (21, 22). Electrophysiological recordings from guinea pig enteric neurons demonstrated that 77% were glucose sensitive (23). Two-thirds of these neurons hyperpolarized (≈5 mV), and their spontaneous electrical discharges were inhibited by the removal of glucose from the extracellular medium. This finding suggests that the modulation of intestinal motor reflexes after a meal is caused by the effects of glucose on these enteric neurons. It was postulated that the glucose sensitivity is mediated by ATP-sensitive K-channels (23). Our results point to a more direct role of glucose through SGLT3, and are reinforced by our observation that the effect of glucose on the mechanical activity of guinea pig ileum is blocked by phlorizin, the specific blocker of SGLT proteins (M. J. Ramirez and A.D.-S., unpublished data).

Although glucose responsive cells are widely distributed throughout the body, from the hypothalamus to endocrine cells (24, 25), little is known about the glucosensors in either animal or plants (1). In yeast, homologs of the facilitated glucose transporters (GLUTs) have been implicated in glucose sensing (2), and this has led to the hypothesis that glucosensors may have evolved from proteins with a glucose-binding site by acquiring a regulatory site for signal transduction (1). Our results suggest that members of the SGLT gene family may also act as glucosensors by conveying information to the cell about the external glucose concentration directly through the membrane potential, or indirectly coupled through another molecule such as a G protein. As glucosensors, the critical factor is not whether the SGLT is a Na^+/glucose cotransporter or a glucose-sensitive ion channel, but where the gene is expressed. The SGLTs are expressed in many different cell types, ranging from epithelia to neurons, and we show here that SGLT3 is in excitable cells. Thus, in skeletal muscle, human, or pig, an increase in glucose concentration will depolarize the membrane either by Na^+/glucose cotransport or by an increased Na^+ conductance through SGLT3.

There is independent evidence that SGLTs are intimately involved in glucosensing in both the central nervous system and gastrointestinal tract. Hypothalamic glucosensing neurons have been implicated in the regulation of food intake and body weight, and these neurons respond to changes in glucose concentration by changes in membrane potential and firing rate (see ref. 26). Although ATP-sensitive K^+ channels may mediate these responses, no changes in ATP concentrations were detected (27). An alternative hypothesis is that SGLTs mediate the change in membrane potential, and this is supported by the observations that phlorizin increases food intake when injected into the cerebrospinal fluid (28, 29) and blocks the glucose-mediated increase in firing rate of glucose-responsive neurons in the hypothalamus (30). Additional evidence comes from studies of glucagon-like peptide-1 secretion from neuroendocrine cells (31). The nonmetabolized sugar αMDG stimulates GLP-1 peptide secretion in a Na^+-dependent and phlorizin-sensitive manner. αMDG increases the membrane conductance, depolarizes the membrane potential, and increases action potential frequency. Although RT-PCR analysis indicated that these neuroendocrine cells express both SGLT1 and SGLT3, the increments in both the electrical activity and GLP-1 secretion at high sugar concentrations suggest a role for SGLT3. The authors concluded that the electrogenic activity of SGLTs provides a novel mechanism for glucose sensing by neuroendocrine cells.

Nature, therefore, seems to be conservative in her approach to the genome: small modifications in structure can result in large changes in function (cotransporter to channel); and changes in the location of gene expression may change the

physiological role (from epithelial transporter to neuronal glucosensor). Successful protein designs may thus be modified to serve diverse purposes, e.g., the SGLTs are cotransporters, uniporters, glucosensors, water channels, and water transporters (32), or the proteins may be expressed in locations where "secondary" functional properties are exploited. All of which emphasizes the limitations of *in silico* projects in assigning function to homologous genes.

Lastly, we comment on the functional differences between the human and pig SGLT3 proteins. When expressed in *X. laevis* oocytes, pig SGLT3 behaves as a low-affinity Na/glucose cotransporter with a greater selectivity for sugars than SGLT1 (5–8, 10). Na^+ and glucose transport are tightly coupled at neutral pH, but at pH 5, ion transport is uncoupled from sugar transport (Fig. 6*C*). Ion transport through human SGLT3 is totally uncoupled from sugar transport at pH 7.5 and 5, but the sugar selectivity of both proteins are quite similar (D-glucose $\approx$ αMDG $\gg$ D-galactose). Thus, the functional differences between human and pig SGLTs are not absolute, but simply a matter of degree and become moot if indeed the pig protein is expressed in cholinergic neurons in the small intestine and at the neuromuscular junction of skeletal muscle.

Sequence alignments of the SGLT genes in general, and hSGLT1, hSGLT3, and pig SGLT3 in particular, provide few positive clues about structural differences that may account for differences in function between the three proteins. This points to the need for caution when extrapolating the function of homologous genes from one to another. Thus, we need to modify the previous interpretation that the uptake of a potential therapeutic agent (β-D-glucosylisophoshoramide) into human tumor cells occurred through SGLT3 (10). We know now that human SGLT3, unlike pig, does not transport the glucoside (not shown) or any other sugar, and so another explanation is needed to account for the observed phlorizin-inhabitable uptake of β-D-glucosylisophoshoramide into tumor cells.

In summary, hSGLT3 is expressed in cholinergic neurons of the small intestine and in skeletal muscle at the neuromuscular junctions, and this, together with the phenotype of hSGLT3 expressed in oocytes, leads to our hypothesis that this membrane protein is a glucosensor involved in the regulation of muscle activity. The pig isoform is also expressed in the small intestine and skeletal muscle, but the cellular location of the protein is unknown. It is also possible that the pig protein is expressed in the enteric nervous system and the neuromuscular junction, where it too behaves as a glucosensor. In this case Na^+/glucose cotransport would also depolarize the membrane potential and thereby regulate muscle activity. This study points to the hitherto unexpected role of SGLTs in regulating muscle activity, and highlights the importance of not only determining the function of new genes in a family but also the cellular location of the protein.

We thank A. Johnson and M. Lai-Bing for the preparation and injection of oocytes, G. A. Zampighi and M. Kreman for the freeze-fracture of the oocytes, Eric Turk for assistance in resequencing the hSGLT3 plasmid, and Eric Turk and K. Philipson for comments on the manuscript. A.D.-S. is a recipient of a postdoctoral fellowship from the American Physiological Society in Physiological Genomics. The work was supported by National Institutes of Health Grants DK44582 and DK19567 and Deutsche Forschungsgemeinschaft Grant SFB487 C1.

1. Rolland, F., Winderickx, J. & Thevelein, J. M. (2001) *Trends Biochem. Sci.* **26,** 310–317.
2. Ozcan, S., Dover, J., Rosenwald, A. G., Wölfl, S. & Johnston, M. (1996) *Proc. Natl. Acad. Sci. USA* **93,** 12428–12432.
3. Loo, D. D. F., Zeuthen, T., Chandy, G. & Wright, E. M. (1996) *Proc. Natl. Acad. Sci. USA* **93,** 13367–13370.
4. Leung, D. W., Loo, D. D. F., Hirayama, B. A., Zeuthen, T. & Wright, E. M. (2000) *J. Physiol.* **528,** 251–257.
5. Mackenzie, B., Panayotova-Heiermann, M., Loo, D. D. F., Lever, J. E. & Wright, E. M. (1994) *J. Biol. Chem.* **269,** 22488–22491.
6. Mackenzie, B., Loo, D. D. F., Panayotova-Heiermann, M. & Wright, E. M. (1996) *J. Biol. Chem.* **271,** 32678–32683.
7. Diez-Sampedro, A., Lostao, M. P., Wright, E. M. & Hirayama, B. A. (2000) *J. Membr. Biol.* **176,** 111–117.
8. Diez-Sampedro, A., Eskandari, S., Wright, E. M. & Hirayama, B. A. (2001) *Am. J. Physiol.* **280,** F278–F282.
9. Dunham, I. Shimizu, N., Roe, B. A., Chissoe, S., Hunt, A. R., Collins, J. E., Bruskiewich, R., Beare, D. M., Clamp, M., Smink, L. J., *et al.* (1999) *Nature* **402,** 489–495.
10. Veyhl, M., Wagner, K., Volk, C., Gorboulev, V., Baumgarten, K., Weber, W. M., Schaper, M., Bertram, B., Wiessler, M. & Koepsell, H. (1998) *Proc. Natl. Acad. Sci. USA* **95,** 2914–2919.
11. Poppe, R., Karbach, U., Gambaryan, S., Wiesinger, H., Lutzenburg, M., Kraemer, M., Witte, O. W. & Koepsell, H. (1997) *J. Neurochem.* **69,** 84–94.
12. Sambrook, J., Fritsch, E. F. & Maniatis, T. (1989) *Molecular Cloning: A Laboratory Manual* (Cold Spring Harbor Lab. Press, Plainview, NY).
13. Valentin, M., Kuhlkamp, T., Wagner, K., Krohne, G., Arndt, P., Baumgarten, K., Weber, W., Segal, A., Veyhl, M. & Koepsell, H. (2000) *Biochim. Biophys. Acta* **1468,** 367–380.
14. Karbach, U., Kricke, J., Meyer-Wentrup, F., Gorboulev, V., Volk, C., Loffing-Cueni, D., Kaissling, B., Bachmann, S. & Koepsell, H. (2000) *Am. J. Physiol.* **279,** F679–F687.
15. Loo, D. D. F., Hirayama, B. A., Gallardo, E. M., Lam, J. T., Turk, E. & Wright, E. M. (1998) *Proc. Natl. Acad. Sci. USA* **95,** 7789–7794.
16. Sasaki, S., Ishibashi, K., Nagai, T. & Marumo, F. (1992) *Biochim. Biophys. Acta* **1137,** 45–51.
17. Kong, C. T., Yet, S. F. & Lever, J. E. (1993) *J. Biol. Chem.* **268,** 1509–1512.
18. Hediger, M. A., Turk, E. & Wright, E. M. (1989) *Proc. Natl. Acad. Sci. USA* **86,** 5748–5752.
19. Zampighi, G. A., Loo, D. D., Kreman, M., Eskandari, S. & Wright, E. M. (1999) *J. Gen. Physiol.* **113,** 507–524.
20. Quick, M., Loo, D. D. F. & Wright, E. M. (2001) *J. Biol. Chem.* **276,** 1728–1734.
21. Kunze, W. A. & Furness, J. B. (1999) *Annu. Rev. Physiol.* **61,** 117–142.
22. Raybould, H. E. & Zittel, T. T. (1995) *Neurogastroenterol. Motil.* **7,** 9–14.
23. Liu, M., Seino, S. & Kirchgessner, A. L. (1999) *J. Neurosci.* **19,** 10305–10317.
24. Ashford, M. L., Boden, P. R. & Treherne, J. M. (1990) *Pflugers Arch.* **415,** 479–483.
25. Kim, M., Cooke, H. J., Javed, N. H., Carey, H. V., Christofi, F. & Raybould, H. E. (2001) *Gastroenterology* **121,** 1400–1406.
26. Levin, B. E. (2001) *Int. J. Obesity* **25,** S68–S72.
27. Ainscow, E. K., Mirshamsi, S., Tang, T., Asford, M. L. J. & Rutter, G. A. (2002) *J. Physiol.* **544,** 429–445.
28. Glick, Z. & Mayer, J. (1968) *Nature* **219,** 1374.
29. Tsujii, S. & Bray, G. A. (1990) *Am. J. Physiol.* **258,** E476–E481.
30. Yang, X.-J., Kow, L.-M., Funabashi, T. & Mobbs, C. V. (1999) *Diabetes* **48,** 1763–1772.
31. Gribble, F. M. Williams, L., Simpson, A. K. & Reimann, F. (2003) *Diabetes* **52,** 1147–1154.
32. Wright, E. M. (2001) *Am. J. Physiol.* **280,** F10–F18.